Effect of Deposition Time on the Structural Properties of RF-Sputtered Aluminum Thin Films

R. Ramos Blazquez[a*], F. Solís-Pomar[a], A. Fundora[b], E. Pérez-Tijerina[a]

[a] *Faculty of Physics and Mathematics, Universidad Autónoma de Nuevo León, San Nicolás de los Garza 66455, Nuevo León, Mexico. ORCID: https://orcid.org/0009-0008-6274-7640*
[b] *Faculty of Physics and Mathematics, Universidad Autónoma de Nuevo León, San Nicolás de los Garza 66455, Nuevo León, Mexico. ORCID: https://orcid.org/0000-0002-4536-6538*
[c] *Higher Institute of Technologies and Applied Sciences, Havana University, Plaza 6163, Cuba. ORCID: https://orcid.org/0000-0001-8809-7529*
[d] *Faculty of Physics and Mathematics, Universidad Autónoma de Nuevo León, San Nicolás de los Garza 66455, Nuevo León, Mexico. ORCID: https://orcid.org/0000-0001-9742-4093*
**email: rramos9708@gmail.com*

Recibido 30 de septiembre 2025, Aceptado 10 octubre 2025

Resumen

Se depositaron películas delgadas de aluminio (Al) sobre sustratos de vidrio BK7 mediante pulverización catódica por radiofrecuencia, variando los tiempos de depósito entre 5 y 20 minutos. Se investigó la influencia de la duración del crecimiento en las propiedades estructurales mediante difracción de rayos X (XRD), revelando que los depósitos más prolongados favorecen el crecimiento de grano y reducen la microdeformación, en concordancia con un mejor orden estructural. El espesor de las películas aumentó linealmente con el tiempo de depósito, obteniéndose una tasa de depósito promedio de 48.1 nm/min. Los tamaños de cristalita estimados por el análisis de Williamson-Hall resultaron superiores a los calculados con la ecuación de Scherrer, lo que resalta la contribución de la deformación al ensanchamiento de los picos. Estos resultados demuestran el ajuste controlado del tiempo de depósito en sputtering permiten una afinación precisa de las características microestructurales de las películas delgadas de Al, lo cual es relevante para optimizar su desempeño en aplicaciones tecnológicas.

Palabras clave: *aluminio, películas delgadas, pulverización catódica, magnetrón, tasa de depósito*

Abstract

Aluminum (Al) thin films were deposited on BK7 glass substrates using radio frequency (RF) magnetron sputtering, with deposition times varied between 5 and 20 minutes. The influence of growth duration on the structural properties was investigated through X-ray diffraction (XRD), revealing that extended deposition promoted grain growth and reduced microstrain, consistent with improved structural ordering. Film thickness increased linearly with deposition time, obtaining an average rate of 48.1 nm/min. Crystallite sizes estimated by Williamson-Hall analysis exceeded those from the Scherrer equation. Highlighting the contribution of strain to peak broadening. These results demonstrate that controlled adjustment of sputtering time enables precise tuning of the microstructural characteristics of Al thin films, relevant for optimizing their performance in technological applications.

Keywords**:** *aluminum, thin films, sputtering, magnetron, deposition rate*

Introduction

In recent years, thin film technology has emerged as a significant area of global research, driving the development of innovative techniques for film growth. Aluminum thin films are widely applied in telecommunications and microelectronics due to their high electrical conductivity, excellent reflectivity, and resistance to corrosion [1]. Among deposition methods, magnetron sputtering has remained a central technique in plasma-based thin film production for more than four decades [2]. This method offers the capability to deposit films over large areas with high rates, strong adhesion, and a reduced environmental footprint compared to chemical processes [3-6].

Pure metals are frequently employed in optical and energy-related applications [7-9]. Aluminum thin films are commonly used as back contacts in solar cells, one main reason for the preference of Al is the low cost, availability and easier fabrication [10]. They are also

used to dope ZnO, enhancing its optoelectronic properties for photodetector applications [11].

Previous studies have shown that, in aluminum-doped thin films produced by RF magnetron sputtering, the optical band gap decreases from 3.48 eV to 3.013 eV as the deposition time increases [12]. In the case of indium tin oxide (ITO) thin films prepared by RF magnetron sputtering, electrical measurements reveal a reduction in resistivity with longer deposition times, attributed to a decrease in carrier concentration [5]. Similarly, for ZnO thin films, increasing thickness results in a reduction of the c-axis lattice parameter and compressive stress, while improving crystallinity on transparent substrates [6].

Establishing the clear relationships between deposition conditions and the resulting properties of thin films is essential to optimize their performance for specific applications. Based on this premise, the present work investigates the influence of deposition time on the structural properties of aluminum thin films.

Methodology

Thin film synthesis

Thin films were deposited by magnetron sputtering onto 25 x 25 mm glass substrates using a 2-inch diameter, 0.25-inch thick aluminum target of 99.99 % purity. The process was conducted in an atmosphere of high-purity argon (99.999%), with an RF power source operating at 13.56 MHz. Prior to deposition, the target was cleaned with a 40 minutes presputtering process, and the substrate surfaces were treated with argon. A base pressure of $3.5*10^{-5}$ Torr was established using a combination of mechanical and turbomolecular pumps, and the working pressure was maintained at $5.0*10^{-3}$ Torr. The target to substrate distance was set at 9 cm. with an argon flow rate of 40 sccm. The RF power was kept at 150 W, while the deposition time was varied. **Table 1** summarizes the specific conditions employed.

Table 1. *Deposition conditions for the Al thin films.*

Deposition time (min)	5, 10, 15, 20
Working pressure (mTorr)	5.0
Ar flux (sccm)	40
RF-power (W)	150
Target-Substrate distance (cm)	9

Characterization

X-ray diffraction (XRD) analysis of the films was performed using an X'Pert³ Powder diffractometer operated at 45 kV and 40 mA, employing Cu Kα radiation (λ = 1.5406 Å). Diffraction patterns were analyzed using the X'Pert HighScore Plus software and identified with reference to the ICCD database. Crystallite sizes were estimated via the Scherrer equation. Microstrain was calculated using the relation:

$$\varepsilon = \frac{\beta}{4\tan\theta}$$

β is the full width at half maximum (FWHM) in radians determined using X'Pert HighScore Plus software and θ is the Bragg angle of the diffraction peak.

To determine the sample thickness, we measured the height difference between the glass substrate and the aluminum film along a 45.5 μm linear scan using an NX10 Atomic Force Microscopy (AFM) from Park Systems Corp., equipped with a SiO_2 tip.

Results and discussion

Crystal structure (XRD)

Figure 1 displays the X-ray diffraction patterns of Al thin films synthesized at different deposition times. The measurements were carried out in a continuous scan mode using a 2θ range from 10^0 to 90^0, with step size=0.026^0 and a fixed incident angle ω=6.0^0.

The crystal structure of the obtained Al thin films corresponds to a face-centered cubic system with space group Fm-3m (PDF 00-004-0787). Observed planes were (1 1 1), (2 0 0), (2 2 0), (3 1 1), and (2 2 2) for all thin films.

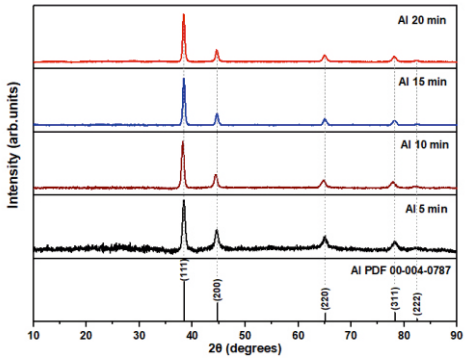

Figure 1. X-Ray diffractograms for the Al thin films obtained at different deposition times.

Figure 2 (a) and (b) present the crystallite size and microstrain values calculated for each diffraction peak, respectively. **Figure 2** (c) provides a comparative plot of these parameters for the most intense peak. As observed, increasing the deposition time results in a gradual increase in crystallite size across all peaks, accompanied by a decrease in microstrain. This trend can be attributed to enhanced grain growth and the relaxation of internal stresses as the film thickness increases. Longer deposition times facilitate the coalescence of crystallites and reduce the density of structural defects, leading to lower microstrain levels in the films [13, 14].

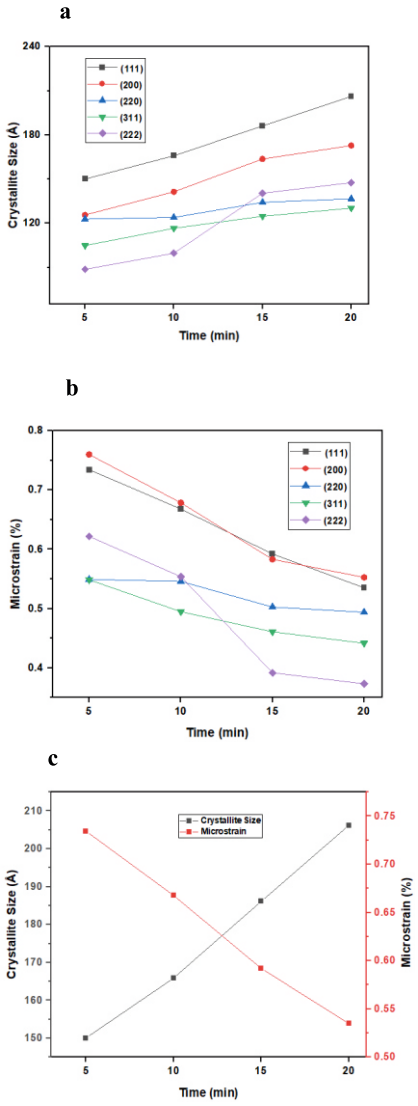

Figure 2. (a) Crystallite size and (b) microstrain calculated for each diffraction peak of the Al thin films deposited at different sputtering times. (c) Comparative analysis of crystallite size and microstrain for the most intense peak.

In addition, we analyzed the crystallite size and microstrain of the samples using the Williamson-Hall (W-H) plot. The W-H method allows the simultaneous estimation of the average crystallite size and microstrain in a material. Unlike the Scherrer equation, which attributes peak broadening solely to the crystallite size, the W-H approach considers both, size and strain contributions [15]. This is achieved by plotting β cos(θ) versus 4 sin(θ), where the intercept provides the crystallite size and the slope gives the microstrain.

The thin films grown at 20 and 15 minutes exhibited the highest crystallite sizes and lowest microstrain values, as previously discussed. For these samples, the W-H method showed high data dispersion, resulting in unreliable linear fitting. This behavior is expected in systems characterized by large grain sizes and minimal internal strain, where the method tends to lose sensitivity and reliability [16, 17]. In such cases, the diffraction peaks are very narrow and small experimental unicertainties can significantly affect the calculation of β, increasing the dispersion of data pointsleading to poor linear correlation or even negative intercepts, which have no physical meaning.

Figure 3 shows the linear fit obtained from the Williamson-Hall analysis for the samples grown at 10 and 5 minutes. The corresponding coefficients of determination (R^2) were 0.90 and 0.81, respectively, indicating a reasonably good fit, especially for the 10 minutes sample. From the intercept and slope of the fitted lines, the estimated crystallite sizes were 332 and 305 nm, and the microstrain values were 0.35% and 0.39% for the films grown at 10 and 5 minutes, respectively. As expected, the crystallite size calculated by the W-H method are higher than those obtained using the Scherrer equation, while for the microstrain values are comparatively lower. This is because the Scherrer equation assumes that all peak broadening arises solely from finite crystallite size. Since the full width at half maximum (β) appears in the denominator of the equation, any additional broadening caused by microstrain leads to an underestaimation of the crystallite size [15, 16]. In contrast, the W-H method separates the contributions, allowing for a more accurate estimation. As a result, the crystallite size appears larger (due to corrected broadening), and the microstrain, when small, yields lower slope values in the linear fit.

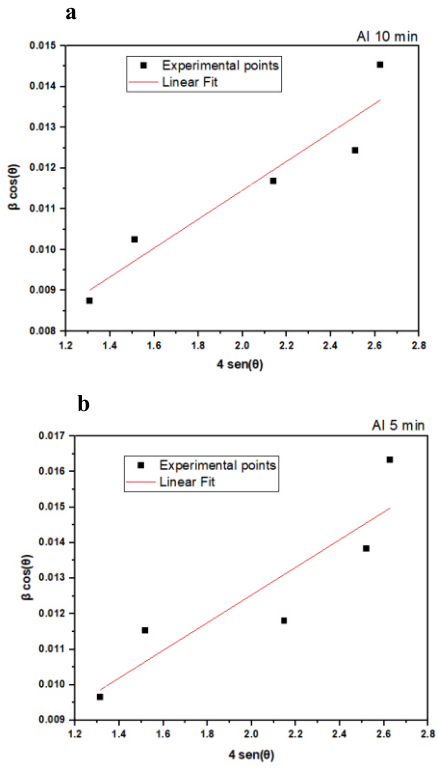

Figure 3. Experimental data and linear fitting of the Williamson-Hall method for the samples grown at: (a) 10 minutes, (b) 5 minutes.

Thin films thickness (AFM)

Table 2 presents the thickness values measured by AFM for each sample deposited at different times. As expected, the film thickness increases with deposition time, since a longer exposure results in more atoms being eroded from the target and subsequently deposited onto the growing film.

Table 2. *Thickness values of aluminum films for samples deposited at different deposition times.*

Deposition time (min)	Thickness (nm)
20	917
15	709
10	404
5	138

Figure 4 (a) displays the optical microscopy view from the AFM for the sample deposited for 10 minutes. The aluminum film appears on the left, and the glass substrate on the right. The corresponding height difference at the interface between the film and the substrate is observed in **Figure 4** (b), yielding a value of 404 nm. It is important to highlight the uniformity of the sputtering process in terms of film thickness. This was confirmed by performing height measurements at different positions across the sample, all showing consistent values.

a

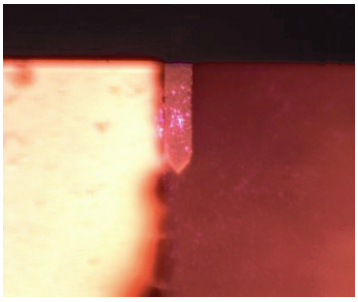

b

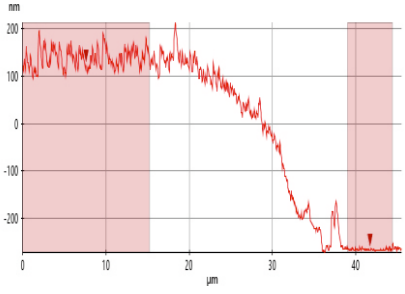

Figure 4. AFM-based thickness analysis of the sample deposited for 10 minutes. (a) Optical view showing the interface between the aluminum film and the glass substrate. (b) Height profile measured along a 45.5 µm linear scan perpendicular to the interface.

Finally, **Figure 5** shows the plot of film thickness versus deposition time. A linear fit was applied to the data, and the slope of the resulting line corresponds to the average deposition rate, which was found to be 48.1± 3.1 nm/min.

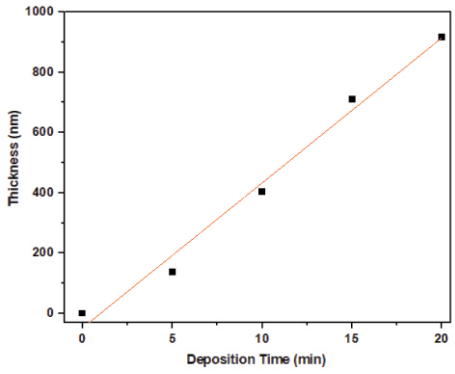

Figure 5. Linear fit to the experimental data obtained for the films thickness of samples deposited at different times.

Conclusions

Al thin films were deposited on BK7 glass substrates by RF magnetron sputtering, with deposition times varied between 5 and 20 minutes. Longer deposition times led to a gradual increase in crystallite size for all diffraction peaks and a concurrent decrease in microstrain, attributed to enhanced grain growth and relaxation of internal stresses with increasing film thickness. The average deposition rate obtained was 48.1 nm/min, and the thickness increase followed a linear behavior. Crystallite sizes obtained from Williamson-Hall analysis were larger than those from the Scherrer equation, as the latter assumes that peak broadening is solely due to finite crystallite size.

References

[1] F.M. Mwema, O.P. Oladimeji, S.A. Akinlabi, E.T. Akinlabi, "Properties of physically deposited thin aluminium film coatings: A review", Journal of Alloys and Compounds 747 (2018) 306-323. https://doi.org/10.1016/j.jallcom.2018.03.006

[2] Gudmundsson, J. T., & Lundin, D. (2020). Introduction to magnetron sputtering. In High power impulse magnetron sputtering, Fundamentals, Technologies, Challenges and Applications (pp. 1-48). https://doi.org/10.1016/B978-0-12-812454-3.00006-1

[3] Li, J., Ren, GK., Chen, J. et al., "Facilitating Complex Thin Film Deposition by Using Magnetron Sputtering: A Review", JOM 74, 3069–3081 (2022). https://doi.org/10.1007/s11837-022-05294-0

[4] A. Baptista, et. al., "Sputtering Physical Vapour Deposition (PVD) Coatings: A Critical Review on Process Improvement and Market Trend Demands", Coatings 2018, 8, 402. https://doi.org/10.3390/coatings8110402

[5] Y. Zhang, et. al., Fabrication of 4.9% efficient Cu2ZnSnS4 solar cell using electron-beam evaporated CdS buffer layer, Thin Solid Films, Volume 685, 2019. https://doi.org/10.1016/j.tsf.2019.06.017

[6] Mendil, D., Challali, F., Touam, T., Chelouche, A., Souici, A. H., Ouhenia, S., & Djouadi, D. (2019). Influence of growth time and substrate type on the microstructure and luminescence properties of ZnO thin films deposited by RF sputtering. Journal of Luminescence, 215, 116631. https://doi.org/10.1016/j.jlumin.2019.116631

[7] A. Baptista, et. al., "Sputtering Physical Vapour Deposition (PVD) Coatings: A Critical Review on Process Improvement and Market Trend Demands", Coatings 2018, 8, 402. https://doi.org/10.3390/coatings8110402

[8] J. Cheng, et al., "Research on magnetron sputtering thin films as electrode materials for supercapacitors", Chemical Engineering Journal, Volume 509, 2025. https://doi.org/10.1016/j.cej.2025.161242

[9] R. Jiang, Y. Da, Z. Chen, X. Cui, X. Han, H. Ke, Y. Liu, Y. Chen, Y. Deng, W. Hu, Progress and Perspective of Metallic Glasses for Energy Conversion and Storage. Adv. Energy Mater. 2022, 12, 2101092. https://doi.org/10.1002/aenm.202101092

[10] F.M. Mwema, E.T. Akinlabi and O.P. Oladijo, Fractal analysis of hillocks: A case of RF sputtered aluminum thin films, Applied Surface Science.

https://doi.org/10.1016/j.apsusc.2019.05.340

[11] B. Wu, et. al., "Tailoring of titanium thin film properties in high power pulsed magnetron sputtering", Vacuum 150 (2018) 144-15. https://doi.org/10.1016/j.vacuum.2018.01.014

[12] A. Iqbal, F. Mohd-Yasin, "Reactive Sputtering of Aluminum Nitride (002) Thin Films for Piezoelectric Applications: A Review", Sensors 2018, 18, 1797. https://doi.org/10.3390/s18061797

[13] Dulmaa, A., Cougnon, F. G., Dedoncker, R., & Depla, D. (2021). On the grain size-thickness correlation for thin films. Acta Materialia, 212, 116896. https://doi.org/10.1016/j.actamat.2021.116896

[14] Devi, K.; Rani, U.; Kumar, A.; Gupta, D.; Aggarwal, S. Tailoring of physical properties of RF-sputtered ZnTe films: role of substrate temperature. Beilstein J. Nanotechnol. **2025,** *16,* 333–348. doi:10.3762/bjnano.16.25

[15] Akl, A. S., & Elhadi, M. (2020). Estimation of crystallite size, lattice parameter, internal strain and crystal impurification of nanocrystalline Al3Ni20Bx alloy by Williamson-Hall method. J. Ovonic Res. https://chalcogen.ro/323_AklAA.pdf

[16] Shishir, M. K. H., Islam, M. M., Islam, M. T., Rahaman, M. A., Mustak, M. H., Mostafa, M. G., & Alam, M. A. (2025). Crystallographic Benchmarking of Powder X-ray Line Diffraction Pattern Profiling of Monoclinic Sucrose Nanocrystal. Results in Surfaces and Interfaces, 100595. https://doi.org/10.1016/j.rsurfi.2025.100595

[17] Gubicza, J. (2022). Reliability and interpretation of the microstructural parameters determined by X-ray line profile analysis for nanostructured materials. The European Physical Journal Special Topics, 231(24), 4153-4165. https://doi.org/10.1140/epjs/s11734-022-00572-z